

**Considering uncertain quantities in the model of cryopreservation process
of biological samples**

Anna Skorupa^{1*}, Alicja Piasecka-Belkhat¹

¹Department of Computational Mechanics and Engineering, Silesian University of Technology, Gliwice, Poland

*Corresponding author: Anna Skorupa, Department of Computational Mechanics and Engineering, Silesian
University of Technology, Gliwice, Poland, e-mail address: anna.skorupa@polsl.pl

Submitted: 26th September 2024

Accepted: 30th January 2025

17 **Abstract**

18 *Purpose:* This paper presents numerical modelling of the heat and mass transfer process in a
19 cryopreserved biological sample. The simulation of the cooling process was carried out
20 according to the liquidus-tracking (LT) protocol developed by Pegg et al., including eight stages
21 in which both the bath solution concentration and temperature are controlled to prevent the
22 formation of ice crystals.

23

24 *Methods:* To determine the temperature distribution during cryopreservation processes, one
25 uses the Fourier equation, while mass transfer was taken into account using an equation based
26 on the Fick's laws. This paper considers a model assuming fuzzy thermophysical parameters
27 described by a triangular and a Gaussian membership function. The numerical problem was
28 solved using the finite difference method including fuzzy set theory.

29

30 *Results:* The diagrams of temperature and mass distributions as a function on time and the
31 distribution of the fuzzy variable at a given moment in time were prepared. Moreover, the fuzzy
32 temperatures and concentrations were compared with experimental results from the literature
33 in table.

34

35 *Conclusions:* In the conclusions, two different types of membership functions were compared
36 with each other, with which the fuzzy variables were described. It can be said that the Gaussian
37 membership function works well for experimental data where the mean and standard deviation
38 are known. In addition, the obtained results were confronted with experimental data. The
39 calculated fuzzy temperatures are consistent with the temperature values occurring in the LT
40 protocol. Larger differences between the experimental data and the calculated values are
41 observed for the fuzzy dimethyl sulfoxide (DMSO) concentration.

42

43

44 **Keywords:** cryopreservation; heat transfer, mass transfer; fuzzy numbers; Gaussian
45 membership function; α -cuts concept

46

47 1. Introduction

48 It is quite common to model biological and engineering processes as deterministic
49 phenomena. However, simulations of physical problems that occur in nature are associated with
50 some uncertainties. They are caused, for example, by the parameters adopted in the model,
51 which are determined experimentally and that the measurements depend on the condition, sex,
52 and quality of the acquired samples 0.

53 Two approaches can be distinguished for considering uncertain variables in the model:
54 probabilistic and non-probabilistic techniques. The first is based on modelling the
55 characteristics of uncertainty through the use of probability distributions that describe how a
56 given random variable might behave. The aim of probabilistic techniques is to predict outcomes
57 under uncertainty. However, their effectiveness is related to access to relevant empirical data
58 obtained for a given parameter, which can be a limitation to their use [23],[29]. On the other
59 hand, non-probabilistic methods include fuzzy set theory and interval set theory. In fuzzy set
60 theory, imprecise variables that are elements of the set are assigned a membership function that
61 determines the degree of membership in the set. The membership function can be described by
62 a linear function, such as a triangular or trapezoidal function, or by more complex relationships,
63 for example, a Gaussian function or a bell function [2],[16],[23]. Fuzzy set theory was first
64 proposed by Zadeh in 1965 [34].

65 Slightly different definitions are given to inaccurate parameters in interval set theory. The
66 interval number is represented by an interval with a given specified lower and upper limit
67 [16],[23]. This concept was invented by Moore in 1966 [19].

68 Let us introduce some information on cryopreservation. This is a process in which the
69 biological activity of biological material is reduced by lowering the temperature. The purpose
70 is to preserve samples in such a way that when they are rewarmed, their physiological activities
71 are restored [31],[35].

72 During cryopreservation, there is a possibility of cell or tissue damage. This is caused, for
73 example, by ice crystallisation or osmotic stress. To eliminate this risk, the cooling (heating)
74 rate is properly regulated and cryoprotective agents (CPAs) are introduced. The most common
75 CPAs are glycerol, dimethyl sulfoxide (DMSO), ethylene glycol, propylene glycol, etc.
76 [11],[12].

77 Depending on the cooling rate and the CPA concentration used, cryopreservation can be
78 performed by different methods. Conventional slow freezing, for example, is characterised by
79 a low cooling rate (approximately 1 °C/min according to Mazur [17]) and a low CPA

80 concentration. Vitrification, on the other hand, involves rapidly cooling the sample to achieve
81 amorphous ice instead of ice crystallisation. This process continues at high CPA concentration
82 [11],[26].

83 Other cryopreservation techniques are worth mentioning. The liquidus-tracking (LT)
84 method, for example, involves controlling the cooling rate and CPA concentration to maintain
85 the temperature in the sample above the melting point, which is altered by the presence of CPA
86 [13],[26].

87 Cryopreservation is a complex multi-physical problem with coupled transport phenomena.
88 The mathematical model includes a description of heat flow and mass transfer associated with
89 molecular diffusion, as well as osmotic transport (microscale process) [15],[26],[31],[33].

90 The paper contains a numerical simulation of the cryopreservation process for a sample made
91 of articular cartilage. The thermal processes occurring during the cryopreservation were
92 examined using the Fourier equation. Furthermore, mass transfer (molecular diffusion) was also
93 analysed applying an equation based on Fick's laws. The study does not consider the
94 phenomenon of osmotic transport. Similar analyses using a deterministic model can be found
95 in the literature [15],[33]. However, there are also uncertainties in the cryopreservation model.
96 Our previous work used interval set theory [22],[24],[26],[27] and fuzzy set theory [23],[26],
97 where a triangular or trapezoidal membership function was introduced. In this study, simulation
98 was performed for fuzzy thermophysical parameters described by a Gaussian membership
99 function, which is a novel approach. The obtained fuzzy results were compared with those for
100 a triangular membership function. For the preparation of the numerical model, the finite
101 difference method (FDM) was implemented.

102 This paper is divided into four chapters. The first chapter provides an introduction, while the
103 second chapter describes the materials selected for the analysis and the methods, which include
104 a heat and mass transfer model and a numerical model. The next chapter presents computational
105 examples. The final chapter contains the conclusions. The study is completed with an Appendix
106 containing the basics of fuzzy numbers and a description of the α -cuts.

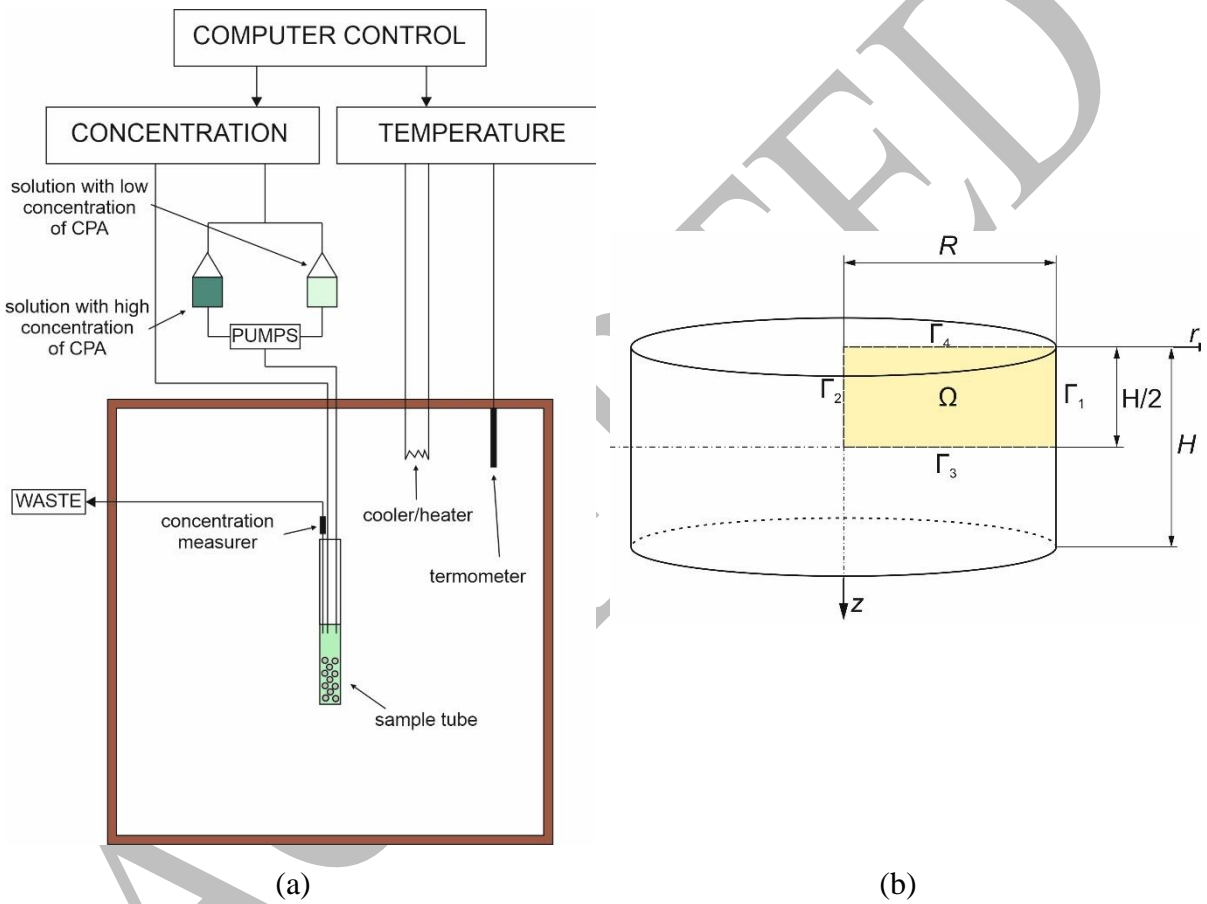
107 2. Methods

108 The study analysed the heat and mass transfer macroscopically in a biological sample during
109 the cryopreservation process. It simulated the cooling process performed according to the LT
110 protocol developed by Pegg et al. [20]. The LT protocol involves eight steps, during which the
111 temperature and concentration of the bath solution are adjusted to prevent the solidification
112 process in the sample by changing its melting point in a controlled manner. The melting point

113 is influenced by CPA, which enters the extracellular matrix of the sample from the bath solution.
 114 Taylor and Hunt [28] and Pegg et al. [20] propose a CPTes2 solution that consisting mainly of
 115 water, DMSO, and also KCl (a potassium-rich mixture). Our research only investigated changes
 116 in the concentration of DMSO.

117 Figure 1a shows a schematic of an example cryopreservation device using the LT protocol
 118 invented by Wang et al. [30]. The study considered the computational domain (Ω) of an
 119 axisymmetric sample (cf. Figure 1b).

120



121 Figure 1. Simplified scheme of device to cryopreservation by LT protocol (a) and scheme of
 122 sample computation domain (b)

123

124 2.1. Heat and mass transfer model

125 Changes in temperature distribution in the computational domain were calculated using the
 126 Fourier equation [3],[8]:

127

$$128 \quad \tilde{c}_V \frac{\partial \tilde{T}(X, t)}{\partial t} = \nabla \cdot (\tilde{k} \nabla \tilde{T}(X, t)) + Q(X, t), \quad (1)$$

129

130 where \tilde{T} is the fuzzy temperature, X refers to the coordinate system, t is the time, Q is the heat
131 source \tilde{c}_V and \tilde{k} represent the fuzzy thermophysical parameters such as the fuzzy volumetric
132 specific heat capacity and fuzzy the thermal conductivity, respectively.

133 For the axisymmetric problem considered in our study, Equation (1) can be expressed:

134

$$135 \quad \tilde{c}_V \frac{\partial \tilde{T}(r,z,t)}{\partial t} = \frac{1}{r} \frac{\partial}{\partial r} \left(\tilde{k} r \frac{\partial \tilde{T}(r,z,t)}{\partial r} \right) + \frac{\partial}{\partial z} \left(\tilde{k} \frac{\partial \tilde{T}(r,z,t)}{\partial z} \right), \quad (2)$$

136

137 where r and z are the cylindrical coordinates. The heat source Q is neglected in further
138 considerations because articular cartilages do not have blood or lymphatic vessels and therefore.

139 The mathematical model of heat transfer was completed for initial-boundary conditions
140 [27],[33]:

141

$$142 \quad \begin{cases} \Gamma_1 \text{ and } \Gamma_4: & -\tilde{k} \mathbf{n} \cdot \nabla \tilde{T}(r, z, t) = \alpha_\Gamma [\tilde{T}(r, z, t) - T_{bath}], \\ \Gamma_2 \text{ and } \Gamma_3: & -\tilde{k} \mathbf{n} \cdot \nabla \tilde{T}(r, z, t) = 0, \\ t = 0 & \tilde{T}(r, z, 0) = T^0, \end{cases} \quad (3)$$

143

144 where \mathbf{n} is the normal vector to the boundary, α_Γ is the natural convection heat transfer
145 coefficient, T_{bath} is the temperature of the surrounding medium (a bathing solution), T_0 is the
146 initial temperature.

147 The relationship describing the mass transfer between external medium and extracellular
148 solutions of the cell, which is named as the molecular diffusion, is the diffusion equation based
149 on Fick's law:

150

$$151 \quad \frac{\partial \tilde{c}_d(X,t)}{\partial t} = \nabla [\tilde{D}(\tilde{T}) \nabla \tilde{c}_d(X, t)], \quad (4)$$

152

153 where \tilde{c}_d is the fuzzy molar concentration, \tilde{D} is the fuzzy molecular diffusion coefficient. The
154 subscript d represents the DMSO as CPA.

155 After conversion of Equation (4) for the axisymmetric problem [3],[6],[7]:

156

$$157 \quad \frac{\partial \tilde{c}_d(r,z,t)}{\partial t} = \frac{1}{r} \frac{\partial}{\partial r} \left(\tilde{D}(\tilde{T}) r \frac{\partial \tilde{c}_d(r,z,t)}{\partial r} \right) + \frac{\partial}{\partial z} \left(\tilde{D}(\tilde{T}) \frac{\partial \tilde{c}_d(r,z,t)}{\partial z} \right). \quad (5)$$

158

159 Please note that the fuzzy diffusion coefficient depends on temperature, which confirms that
 160 the mathematical model of cryopreservation represents a multi-physics coupled problem . The
 161 diffusion coefficient can be calculated from the Einstein-Stokes equation [4],[18]:

$$162 \quad \quad \quad 163 \quad \quad \quad \tilde{D}(\tilde{T}) = \frac{k_B \tilde{T}(r,z,t)}{6\pi r_s \mu}, \quad (6)$$

164 where k_B is the Boltzmann constant ($k_B = 1.38 \times 10^{-23} \text{ J}\cdot\text{K}^{-1}$), r_s is the radius of the spherical
 165 particle, μ is the dynamic viscosity.

166 **The mass transport model also includes initial-boundary conditions [27]:**

$$167 \quad \quad \quad 168 \quad \quad \quad \begin{cases} \Gamma_1 \text{ and } \Gamma_4: & \tilde{c}_d(r, z, t) = 0.9c_{bath}, \\ \Gamma_2 \text{ and } \Gamma_3: & -\mathbf{n} \cdot \tilde{D}(\tilde{T})\nabla\tilde{c}_d(r, z, t) = 0, \\ t = 0: & \tilde{c}_d(r, z, 0) = c^0, \end{cases} \quad (7)$$

169 where c^0 is the initial concentration, c_{bath} is the concentration of the surrounding medium (a
 170 bathing solution). The 0.9 factor reflects the mass transfer between the domain Ω and the
 171 surrounding medium.
 172
 173

174 2.2. Numerical model

175 The numerical model was prepared applying the finite difference method (FDM) considering
 176 fuzzy numbers theory (see Appendix). An explicit scheme was used to analyse transport
 177 phenomena for unsteady state [18].

178 A time mesh was established with a constant step, defined by $\Delta t = t^{j-1} - t^j$. The grid for
 179 computational domain (Ω) was created based on the five-point star illustrated schematically in
 180 Figure 2, where h_1 and h_2 represent the mesh step in the r - and z -direction, respectively, node
 181 (i, j) is the central node. **This concept assumes that boundary nodes are located at a distance of**
 182 **$0.5h_1$ and $0.5h_2$ from the edge. [18].**

183

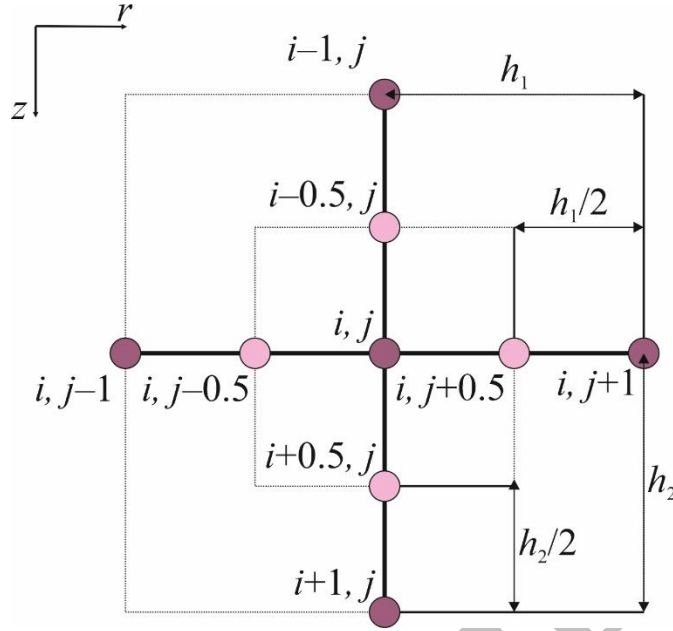


Figure 2. Five-points star

184

185

186

187 The idea of FDM is to convert differential equations into algebraic equations by replacing
 188 the appropriate differential quotients. Different types of differential quotients can be consulted
 189 in the literature [26].

190 By substituting the relevant relations into Equation (2), and after transformation, the
 191 following formula for internal nodes was obtained [26]:

192

$$193 \quad \tilde{T}_{i,j}^f = \tilde{T}_{i,j}^{f-1} + \frac{\Delta t}{\tilde{c}_V} \left[\sum_{a=1}^4 \frac{\Phi_e}{\tilde{R}_e^{f-1}} (\tilde{T}_e^{f-1} - \tilde{T}_{i,j}^{f-1}) \right], \quad (8)$$

194

195 where $i = 2, 3, \dots, n-1$ and $j = 2, 3, \dots, m-1, n$ and m are the number of nodes, a corresponds
 196 to $e = \{(i, j+1); (i, j-1); (i+1, j); (i-1, j)\}$, \tilde{R}_e and Φ_e is the fuzzy thermal resistance and the
 197 shape function, respectively, where:

198

$$199 \quad \begin{aligned} \tilde{R}_{i,j-1}^{f-1} &= \frac{0.5h_1}{\tilde{k}_{i,j}^{f-1}} + \frac{0.5h_1}{\tilde{k}_{i,j-1}^{f-1}}, & \tilde{R}_{i,j+1}^{f-1} &= \frac{0.5h_1}{\tilde{k}_{i,j}^{f-1}} + \frac{0.5h_1}{\tilde{k}_{i,j+1}^{f-1}}, \\ \tilde{R}_{i-1,j}^{f-1} &= \frac{0.5h_2}{\tilde{k}_{i,j}^{f-1}} + \frac{0.5h_2}{\tilde{k}_{i-1,j}^{f-1}}, & \tilde{R}_{i+1,j}^{f-1} &= \frac{0.5h_2}{\tilde{k}_{i,j}^{f-1}} + \frac{0.5h_2}{\tilde{k}_{i+1,j}^{f-1}}, \end{aligned} \quad (9)$$

200

201 and

202

$$203 \quad \Phi_{i,j-1} = \frac{r_{i,j-0.5h_1}}{r_{i,j}h_1}, \quad \Phi_{i,j+1} = \frac{r_{i,j+0.5h_1}}{r_{i,j}h_1}, \quad \Phi_{i-1,j} = \Phi_{i+1,j} = \frac{1}{h_2}, \quad (10)$$

204

205 where $r_{i,j}$ is the radial coordinate of the node (i, j) .206 In a similar procedure, a numerical model was created for the mass transfer, hence Equation
207 (5) for internal nodes has the form [26]:

208

209
$$(\tilde{c}_d)_{i,j}^f = (\tilde{c}_d)_{i,j}^{f-1} + \Delta t \sum_{a=1}^4 \frac{\Phi_e}{\tilde{W}_e^{f-1}} [(\tilde{c}_d)_e^{f-1} - (\tilde{c}_d)_{i,j}^{f-1}], \quad (11)$$

210

211 where $i = 2, 3, \dots, n - 1$ and $j = 2, 3, \dots, m - 1$, \tilde{W}_e is the fuzzy mass diffusion resistance:

212

213
$$\begin{aligned} \tilde{W}_{i,j-1}^{f-1} &= \frac{0.5h_1}{\tilde{D}_{i,j}^{f-1}} + \frac{0.5h_1}{\tilde{D}_{i,j-1}^{f-1}}, & \tilde{W}_{i,j+1}^{f-1} &= \frac{0.5h_1}{\tilde{D}_{i,j}^{f-1}} + \frac{0.5h_1}{\tilde{D}_{i,j+1}^{f-1}}, \\ \tilde{W}_{i-1,j}^{f-1} &= \frac{0.5h_2}{\tilde{D}_{i,j}^{f-1}} + \frac{0.5h_2}{\tilde{D}_{i-1,j}^{f-1}}, & \tilde{W}_{i+1,j}^{f-1} &= \frac{0.5h_2}{\tilde{D}_{i,j}^{f-1}} + \frac{0.5h_2}{\tilde{D}_{i+1,j}^{f-1}}. \end{aligned} \quad (12)$$

214

215 The implementation of differential quotients for boundary nodes was reported in the
216 literature [26], therefore this element of the numerical model will not be presented here.

217 A stability condition was also specified for the given model [26]:

218

219
$$\Delta t \leq \sum_{a=1}^4 \frac{\tilde{R}_e^{f-1}}{\Phi_e} \quad \text{and} \quad \Delta t \leq \sum_{a=1}^4 \frac{\tilde{W}_e^{f-1}}{\Phi_e}. \quad (13)$$

220

3. Results

221 **Our study modelled the cryopreservation process for a homogeneous biological sample made**
222 **of articular cartilage with dimensions $H = 1 \times 10^{-3}$ m and $R = 3 \times 10^{-3}$ m (see Figure 1b).** The
223 thermophysical parameters were introduced as fuzzy numbers described by a triangular
224 function and a Gaussian function. For the analysis for triangular fuzzy numbers, the following
225 parameter values were introduced: $\tilde{c}_v = (3.728 \times 10^6; 3.924 \times 10^6; 4.120 \times 10^6) \text{ J} \cdot \text{K}^{-1} \cdot \text{m}^{-3}$ and $\tilde{k} =$
226 $(0.492; 0.518; 0.544) \text{ W} \cdot \text{m}^{-1} \cdot \text{K}^{-1}$. For Gaussian fuzzy number, it was assumed that: the mean
227 values are $m_{cv} = 3.924 \times 10^6 \text{ J} \cdot \text{K}^{-1} \cdot \text{m}^{-3}$, $m_k = 0.518 \text{ W} \cdot \text{m}^{-1} \cdot \text{K}^{-1}$ and standard deviations are $\sigma_{cv} =$
228 $1.962 \times 10^4 \text{ J} \cdot \text{K}^{-1} \cdot \text{m}^{-3}$, $\sigma_k = 0.026 \text{ W} \cdot \text{m}^{-1} \cdot \text{K}^{-1}$ for the volumetric specific heat capacity and the
229 thermal conductivity, respectively [1],[32],[33]. Convection heat transfer coefficient is equal to
230 $\alpha_\Gamma = 525 \text{ W} \cdot \text{m}^{-2} \cdot \text{K}^{-1}$ [33]. Other parameters used in the simulation were input data characterizing
231 the chemical properties of CPA (DMSO) in the context of the diffusion phenomenon, which
232 are $r_s = 2.541 \cdot 10^{-10} \text{ m}$ and $\mu = 1.996 \cdot 10^{-3} \text{ Pa} \cdot \text{s}$ [25],[33].

233 The model was completed with initial conditions, where $T^0 = 22 \text{ }^\circ\text{C}$, $c^0 = 0 \text{ } \%(w/w)$ [27],[33].
 234 However, the values of temperature and DMSO concentration of the bath solution used to
 235 calculate the boundary variables are determined based on Pegg's protocol for cooling, as shown
 236 in Table 1 [20].

237 For the fuzzy numbers described by the triangular membership function, the simulations
 238 were performed for $\alpha = \{0; 0.25; 0.5; 0.75; 1\}$, while for the fuzzy numbers described by the
 239 Gauss membership function, for $\alpha = \{0.001; 0.15; 0.25; 0.35; 0.45; 0.5; 0.65; 0.75; 0.85; 0.95;$
 240 $1\}$. It is also assumed that time step $\Delta t = 0.005 \text{ s}$ and mesh steps $h_1 = 0.0001 \text{ m}$ and $h_2 = 0.00005$
 241 m .

242

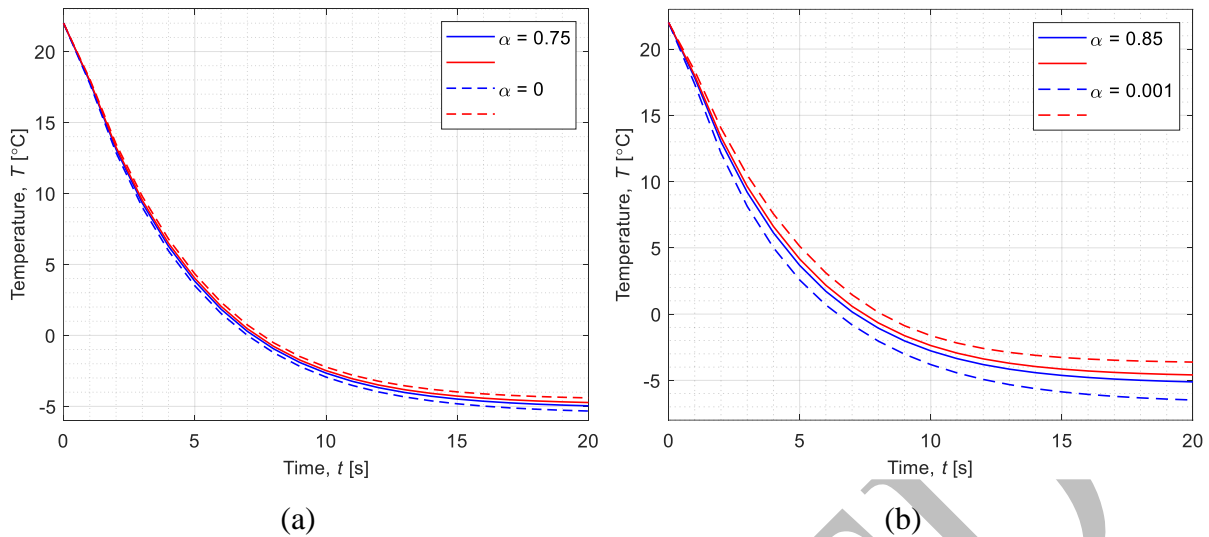
243 Table 1. Temperature and DMSO concentration of the bath solution

Step	Time duration	Temperature of Bath Solution	Concentration of Bath Solution
	$t \text{ [min]}$	$T_{bath} \text{ [}^\circ\text{C]}$	$c_{bath} \text{ [} \%(w/w) \text{]}$
1.	10	22	10
2.	10	22	20
3.	30	-5	29
4.	30	-8.5	38
5.	30	-16	47
6.	30	-23	56
7.	30	-35	63
8.	30	-48.5	72

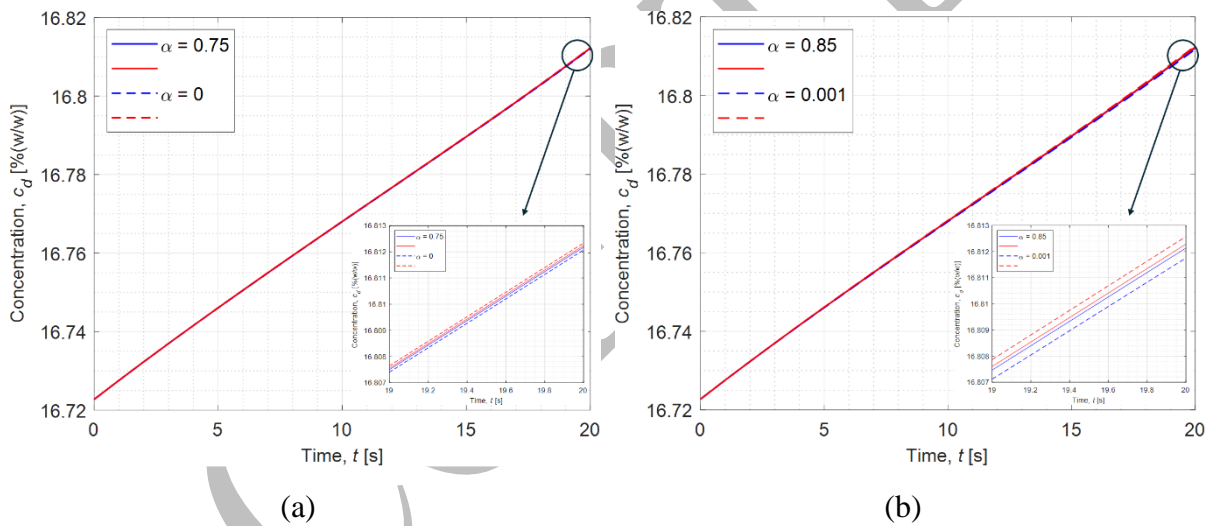
244

245 Figures 3-6 show the results of the simulation, which were collected at point $r = 0.00005 \text{ m}$,
 246 $z = 0.000475 \text{ m}$. Figure 3 illustrates the fuzzy temperature curves in the selected period of time
 247 (for 20 s of step 3) for different parameters α using triangular (a) and Gaussian (b) membership
 248 function. Figure 4, in analogy to Figure 3, presents the dependence of the fuzzy concentration
 249 of DMSO over a selected period of time (for 20 s of step 3). for different parameters α using
 250 triangular (a) and Gaussian (b) membership function.

251



252 **Figure 3. Fuzzy temperature in time (for 20 s of step 3, point $r = 5 \times 10^{-5}$ m,**
 253 **$z = 4.75 \times 10^{-4}$ m) for triangular (a) and Gaussian (b) membership functions**

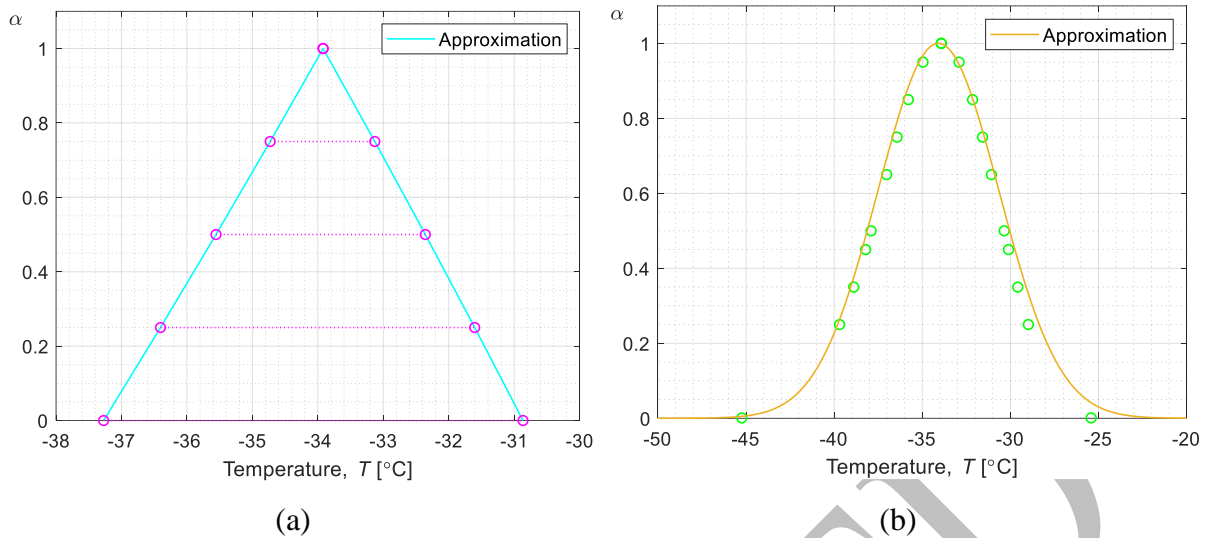


255 **Figure 4. Fuzzy concentration in time (for 20 s of step 3, point $r = 5 \times 10^{-5}$ m,**
 256 **$z = 4.75 \times 10^{-4}$ m) for triangular (a) and Gaussian (b) membership functions**

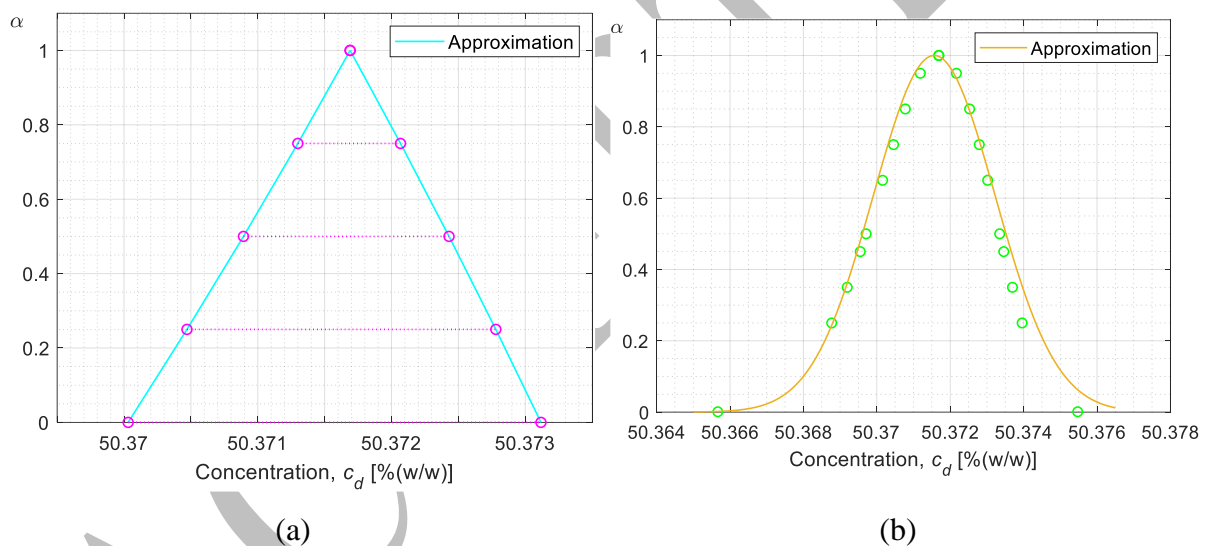
257
 258 **1.**

259 Figure 5 depicts the fuzzy temperature at the selected moment of simulation time (10 s at
 260 step 7) obtained for the triangular (a) and Gaussian (b) membership functions. Please note that
 261 the distribution of the variable was approximated from the results for the Gaussian membership
 262 function. Similarly, Figure 6 shows the fuzzy DMSO concentration at a selected moment of
 263 simulation time (10 s at step 7) received for the triangular (a) and Gaussian (b) membership
 264 functions.

265



266 **Figure 5. Fuzzy temperature at the selected moment of simulation time (10 s at step 7, point**
 267 **$r = 5 \times 10^{-5}$ m, $z = 4.75 \times 10^{-4}$ m) for the triangular (a) and Gaussian (b) membership functions**
 268



269 **Figure 6. Fuzzy concentration at the selected moment of simulation time (10 s at step 7, point**
 270 **$r = 5 \times 10^{-5}$ m, $z = 4.75 \times 10^{-4}$ m) for the triangular (a) and Gaussian (b) membership functions**
 271

272 Table 2 compares the obtained concentration for the triangular and Gaussian membership
 273 functions with the experimental data from the literature [20]. The first two columns show the
 274 obtained fuzzy temperature results for the triangular and Gaussian membership functions. It can
 275 be seen that the given fuzzy temperatures coincide with the bath solution temperatures (compare
 276 with Table 1). The next sections of the table show a comparison of the fuzzy DMSO
 277 concentration in the cellular matrix described by the triangular and Gaussian membership
 278 functions with the experimental results. For the DMSO concentration, there are differences
 279 between the simulation results and the experimental data, as shown by the calculated relative

280 error, the highest value of which is 15.82% (step 8) and the lowest value of which is 0.06%
 281 (step 4).

282

283 **Table 2. Comparison of results with experimental data**

Step	Fuzzy temperature for $\alpha = 0$ (triangular m. f.), \tilde{T} [°C]	Fuzzy temperature (Gaussian m. f.), \tilde{T} [°C]	Fuzzy concentration for $\alpha = 0$ (triangular m. f.), \tilde{c}_d [% (w/w)]	Fuzzy concentration (Gaussian m. f.), \tilde{c}_d [% (w/w)]	Experimental data, c_d [% (w/w)]	Relative error, δ [%]
1	[22.0000; 22.0000]	$m = 22.0000$ $\sigma = 0.0000$	[7.8386; 7.8386]	$m = 7.8386$; $\sigma = 0.0000$	–	–
2	[22.0000; 22.0000]	$m = 22.0000$ $\sigma = 0.0000$	[16.7228; 16.7228]	$m = 16.7228$ $\sigma = 0.0000$	16.3 ± 1.3	2.59
3	[-5.5120; -4.5355]	$m = -5.0454$ $\sigma = 0.6996$	[26.0787; 26.0792]	$m = 26.0790$ $\sigma = 3.55 \times 10^{-4}$	24.5 ± 1.1	6.44
4	[-9.3704; -7.7104]	$m = -8.5773$ $\sigma = 1.1893$	[34.1789; 34.1798]	$m = 34.1793$ $\sigma = 5.95 \times 10^{-4}$	34.2 ± 0.9	0.06
5	[-17.6384; -14.5136]	$m = -16.1454$ $\sigma = 2.2386$	[42.2743; 42.2762]	$m = 42.2752$ $\sigma = 0.0013$	41.7 ± 3.3	1.38
6	[-25.3552; -20.8633]	$m = -23.2090$ $\sigma = 3.2180$	[50.3691; 50.3722]	$m = 50.3705$ $\sigma = 0.0023$	47.8 ± 2.8	5.38
7	[-38.5840; -31.7485]	$m = -35.3181$ $\sigma = 4.8969$	[56.6669; 56.6719]	$m = 56.6692$ $\sigma = 0.0037$	52.2 ± 1.3	8.56
8	[-53.4664; -43.9944]	$m = -48.9408$ $\sigma = 6.7857$	[64.7393; 64.7516]	$m = 64.7449$ $\sigma = 0.0093$	55.9 ± 2.9	15.82

284 m. f. – membership function

285 **4. Discussion**

286 To begin with, it is worth examining the results in Figures 3-6 and the Table 2. It can be seen
 287 that the temperature distribution in the sample stabilises relatively quickly and reaches the value
 288 of the bath solution (cf. Figure 3). In the case of a change in DMSO concentration, a continuous
 289 increase is observed without any apparent stabilisation as in the case of the temperature curve
 290 (cf. Figure 4). In addition, it is noticeable in the graphs in Figures 3 and 4 that the smaller the
 291 value of the parameter α , the narrower the width of the interval. From Figures 5 and 6 it can
 292 also be observed that the value of parameter α affects the width of the interval. Similar

293 conclusions about the effect of the parameter α on the distribution of a given quantity described
294 as a fuzzy number are provided, for example, in the dissertation [26]. This thesis considers
295 different computational problems for the cryopreservation process applying fuzzy numbers
296 described by triangular and trapezoidal membership functions.

297 In this study, numerical simulations were performed for fuzzy thermophysical parameters
298 described by a Gaussian membership function, which is a novel approach (in [21],[23],[26]
299 only the triangular and trapezoidal membership function are presented). The results obtained
300 were compared with those for the triangular membership function (see Table 2 and Figures 5-
301 6). Triangular fuzzy numbers have sharp and linear membership boundaries, which makes them
302 easier to implement. The Gaussian membership function, on the other hand, has smooth
303 boundaries and tends asymptotically to zero. Gaussian fuzzy numbers are more complex to
304 calculate due to the exponential nature of the membership function. It can be assumed that it is
305 worth using them to model probabilistic phenomena. The use of Gaussian fuzzy numbers is
306 certainly an interesting extension of the research topic dealt with by the authors of this paper.

307 On the other hand, analysing Table 2, it is noticeable discrepancies between numerical results
308 and experimental data. Referring to previous articles, it can be suggested that it is worthwhile
309 to analyse, for example, the mathematical model, the calculated values of the diffusion
310 coefficient, as well as the introduced thermophysical parameters. A similar study of
311 cryopreservation using the LT protocol and the deterministic thermophysical parameters
312 presents Yu et al. [33]. However, Yu et al. in their assumptions determined that the extracellular
313 matrix of articular cartilage is a porous and isotropic material. As a consequence, the diffusion
314 coefficient depends on the properties of the porous media, such as the tortuosity. This
315 assumption can consequently lead to more accurate numerical simulation results. Articular
316 cartilage as a porous material is also described in the work of Behrou et al. [1], who distinguish
317 the liquid and solid phases in the tissue, and explore the effect of temperature on its properties.

318

319 **5. Conclusion**

320 This paper presents the results of a simulated cryopreservation of a biological sample. The
321 cryopreservation of an articular cartilage sample was modelled using the LT protocol. This
322 approach allows the temperature and concentration to be controlled in order to avoid the
323 formation of ice crystals which would lead to the destruction of the biological sample. Due to
324 the imprecise nature of the thermophysical parameters, they were introduced as fuzzy numbers
325 described by a triangular and a Gaussian membership function. It should be noted that Gaussian

326 fuzzy numbers do not have the sharp interval boundaries that characterise triangular numbers.
 327 Therefore, the Gaussian membership function works well for experimental data where the mean
 328 and standard deviation are known. Triangular and Gaussian fuzzy numbers also share common
 329 characteristics. Using the α -cut concept, the width of the interval is widest for $\alpha = 0$ and
 330 narrowest for $\alpha = 1$ (is equal to 0).

331 The obtained fuzzy concentrations and temperatures in eight stages of the LT protocol for
 332 triangular and Gaussian membership functions were compared with experimental data taken
 333 from the literature. The calculated fuzzy temperatures are consistent with the temperature
 334 values occurring in the LT protocol. Larger differences between the experimental data and the
 335 calculated values are observed for the fuzzy DMSO concentration, where the maximum relative
 336 error is 15.82%. It is suggested that this is due to an inappropriate selection of thermophysical
 337 parameters or a model describing the diffusion coefficient.

338 Acknowledgment

339 The research was partially funded from financial resources from the statutory subsidy of the
 340 Faculty of Mechanical Engineering, Silesian University of Technology

341 Appendix

342 Sets \tilde{A} of fuzzy numbers are sets in which each element x is assigned a relevant membership
 343 function [5],[9],[21]:

$$344 \quad \tilde{A} = \{(x, \mu_{\tilde{A}}(x)); x \in \mathbb{X}\}, \quad (A.1)$$

345 where $\mu_{\tilde{A}}$ is the membership function, which takes the value from 0 to 1. Fuzzy numbers which
 346 belong to a set can be described by different membership functions. In our study, the triangle
 347 membership function described as a straight line and the Gaussian membership function were
 348 implemented.

349 The membership function for the triangular fuzzy number $\tilde{a} = (a^-, a_0, a^+)$ is expressed by
 350 the relation [10],[21]:

$$351 \quad \mu_{\tilde{a}}(x) = \begin{cases} 0, & x < a^-, \\ \frac{x-a^-}{a_0-a^-}, & a^- \leq x \leq a_0, \\ \frac{a^+-x}{a^+-a_0}, & a_0 \leq x \leq a^+, \\ 0, & x > a^+, \end{cases} \quad (A.2)$$

355

356 where a_0 , a^- , a^+ are the core of the number and the left and right ends of the fuzzy number,
357 respectively.

358 On the other hand, the Gaussian membership function for a fuzzy number $\tilde{a} = (m_a, \sigma_a)$ has
359 the form [14]:

360

$$361 \quad \mu_{\tilde{a}}(x) = \exp\left[\frac{-(x-m_a)^2}{2\sigma_a^2}\right], \quad (\text{A.3})$$

362

363 where m_a , σ_a denote the mean value and standard deviation of data set a , respectively.

364 The α -cut for a given fuzzy set \tilde{A}_α is defined as the set of all elements \tilde{A} whose membership
365 function is greater than α [5],[10]:

366

$$367 \quad \tilde{A}_\alpha = \{x \in \mathbb{X}: \mu_{\tilde{A}}(x) \geq \alpha\}. \quad (\text{A.4})$$

368

369 As a consequence, a fuzzy number is calculated as the sum of all α -cuts:

370

$$371 \quad \tilde{A} = \sum_{\alpha \in [0,1]} \alpha \tilde{A}_\alpha. \quad (\text{A.5})$$

372

373 Then the fuzzy numbers are expressed as closed intervals, where for triangular fuzzy
374 numbers it is given as [21]:

375

$$376 \quad \tilde{a}_\alpha = [(a_0 - a^-)\alpha + a^-, (a_0 - a^+)\alpha + a^+], \quad (\text{A.6})$$

377

378 and for fuzzy numbers described by Gaussian membership function [14]:

379

$$380 \quad \tilde{a}_\alpha = [m_a - \sigma_a \sqrt{-2 \ln \alpha}, m_a + \sigma_a \sqrt{-2 \ln \alpha}]. \quad (\text{A.7})$$

381 Literature

- 382 [1] Behrou R., Foroughi H., Haghpanah F., Numerical study of temperature effects on the
383 poro-viscoelastic behavior of articular cartilage, Journal of the Mechanical Behavior of
384 Biomedical Materials, 2018, 78, pp. 214–223, DOI: 10.1016/j.jmbbm.2017.11.023.
385 [2] Caniani D., Lioi D.S., Mancini I.M., Masi S., Application of fuzzy logic and sensitivity
386 analysis for soil contamination hazard classification, Waste Management, 2011, 31(3),
387 pp. 583–594, DOI: 10.1016/j.wasman.2010.09.012.

- 388 [3] Çengel Y.A., Ghajar A.J., Heat and mass transfer: fundamentals and applications.
389 McGraw-Hill Higher Education, 2015.
- 390 [4] Cichocki B., Albert Einstein – praca o ruchach Browna z 1905 roku, *DeltaMi*, 2005.
391 [http://www.deltami.edu.pl/temat/fizyka/struktura_materii/2011/01/01/Albert_Einstein-](http://www.deltami.edu.pl/temat/fizyka/struktura_materii/2011/01/01/Albert_Einstein-praca_o_ruchach/)
392 [praca_o_ruchach/](http://www.deltami.edu.pl/temat/fizyka/struktura_materii/2011/01/01/Albert_Einstein-praca_o_ruchach/) (accessed Aug. 02, 2022).
- 393 [5] Dubois D.J., Fuzzy Sets and Systems: Theory and Applications. Academic Press, 1980.
- 394 [6] Fick A., Ueber Diffusion, *Annalen der Physik*, 1855, 94(1), pp. 59–86, DOI:
395 10.1002/andp.18551700105.
- 396 [7] Fick A., V. On liquid diffusion, *Philosophical Magazine*, 1855, 10(63), pp. 30–39, DOI:
397 10.1080/14786445508641925.
- 398 [8] Fourier J.B.J., *Théorie analytique de la chaleur*. Firmin Didot, 1882.
- 399 [9] Hanss M., *Applied Fuzzy Arithmetic*. Springer Berlin Heidelberg New York, 2005.
- 400 [10] Hatłas M., *Modelling and optimisation of inhomogeneous materials using granular*
401 *computations*, Doctoral thesis, Politechnika Śląska, Gliwice, 2021.
- 402 [11] Jang T.H. *et al.*, Cryopreservation and its clinical applications, *Integrative Medicine*
403 *Research*, 2017, 6(1), pp. 12–18, DOI: 10.1016/j.imr.2016.12.001.
- 404 [12] Jungare K.A., Radha R., Sreekanth D., Cryopreservation of biological samples – A short
405 review, *Materials Today: Proceedings*, 2022, 51, pp. 1637–1641, DOI:
406 10.1016/j.matpr.2021.11.203.
- 407 [13] Kay A.G., Hoyland J.A., Rooney P., Kearney J.N., Pegg D.E., A liquidus tracking
408 approach to the cryopreservation of human cartilage allografts, *Cryobiology*, 2015,
409 71(1), pp. 77–84, DOI: 10.1016/j.cryobiol.2015.05.005.
- 410 [14] Leandry L., Sosoma I., Koloseni D., Basic Fuzzy Arithmetic Operations Using α -Cut for
411 the Gaussian Membership Function, *Journal of Fuzzy Extension and Applications*, 2022,
412 3(4), pp. 337–348, DOI: 10.22105/jfea.2022.339888.1218.
- 413 [15] Liu W., Zhao G., Shu Z., Wang T., Zhu K., Gao D., High-precision approach based on
414 microfluidic perfusion chamber for quantitative analysis of biophysical properties of cell
415 membrane, *International Journal of Heat and Mass Transfer*, 2015, 86, pp. 869–879,
416 DOI: 10.1016/j.ijheatmasstransfer.2015.03.038.
- 417 [16] Lü H., Shangguan W.-B., Yu D., Uncertainty quantification of squeal instability under
418 two fuzzy-interval cases, *Fuzzy Sets and Systems*, 2017, 328, pp. 70–82, DOI:
419 10.1016/j.fss.2017.07.006.
- 420 [17] Mazur P., Kinetics of Water Loss from Cells at Subzero Temperatures and the Likelihood
421 of Intracellular Freezing, *Journal of General Physiology*, 1963, 47(2), pp. 347–369, DOI:
422 10.1085/jgp.47.2.347.
- 423 [18] Mochnecki B., Suchy J., *Modelowanie i symulacja krzepnięcia odlewów*. Warszawa:
424 Wydawnictwo Naukowe PWN, 1993.
- 425 [19] Moore R.E., *Interval Analysis*. New Jersey, USA: Printice-Hall, 1966.
- 426 [20] Pegg D.E., Wang L., Vaughan D., Cryopreservation of articular cartilage. Part 3: The
427 liquidus-tracking method, *Cryobiology*, 2006, 52(3), pp. 360–368, DOI:
428 10.1016/j.cryobiol.2006.01.004.
- 429 [21] Piasecka-Belkhat A., *Przedziałowa metoda elementów brzegowych w nieprecezyjnych*
430 *zadaniach nieustalonej dyfuzji ciepła*. Gliwice: Wydawnictwo Politechniki Śląskiej,
431 2011.
- 432 [22] Piasecka-Belkhat A., Skorupa A., Application of interval arithmetic in numerical
433 modeling of cryopreservation process during cryoprotectant loading to microchamber,
434 *Numerical Heat Transfer, Part A: Applications*, 2022, 84(2), pp. 83–101, DOI:
435 10.1080/10407782.2022.2105078.

- 436 [23] Piasecka-Belkhat A., Skorupa A., Cryopreservation analysis considering degree of
437 crystallisation using fuzzy arithmetic, *Journal of Theoretical and Applied Mechanics*,
438 2024, pp. 207–218, DOI: 10.15632/jtam-pl/183697.
- 439 [24] Piasecka-Belkhat A., Skorupa A., Numerical Study of Heat and Mass Transfer during
440 Cryopreservation Process with Application of Directed Interval Arithmetic, *Materials*,
441 2021, 14(11), p. 2966, DOI: 10.3390/ma14112966.
- 442 [25] Schulze B.M., Watkins D.L., Zhang J., Ghiviriga I., Castellano R.K., Estimating the
443 shape and size of supramolecular assemblies by variable temperature diffusion ordered
444 spectroscopy, *Org. Biomol. Chem.*, 2014, 12(40), pp. 7932–7936, DOI:
445 10.1039/C4OB01373E.
- 446 [26] Skorupa A., *Multi-scale modelling of heat and mass transfer in tissues and cells during*
447 *cryopreservation including interval methods*, Doctoral thesis, Politechnika Śląska,
448 Gliwice, 2023. Accessed: Oct. 10, 2023. [Online]. Available:
449 <https://repolis.bg.polsl.pl/dlibra/publication/85590/edition/76693>
- 450 [27] Skorupa A., Piasecka-Belkhat A., Numerical Modeling of Heat and Mass Transfer
451 during Cryopreservation Using Interval Analysis, *Applied Sciences*, 2020, 11(1), p. 302,
452 DOI: 10.3390/app11010302.
- 453 [28] Taylor M.J., Hunt C.J., A new preservation solution for storage of corneas at low
454 temperatures, *Current Eye Research*, 1985, 4(9), pp. 963–973, DOI:
455 10.3109/02713689509000003.
- 456 [29] Wang C., Matthies H.G., Coupled fuzzy-interval model and method for structural
457 response analysis with non-probabilistic hybrid uncertainties, *Fuzzy Sets and Systems*,
458 2021, 417, pp. 171–189, DOI: 10.1016/j.fss.2020.06.002.
- 459 [30] Wang L., Pegg D.E., Lorrison J., Vaughan D., Rooney P., Further work on the
460 cryopreservation of articular cartilage with particular reference to the liquidus tracking
461 (LT) method, *Cryobiology*, 2007, 55(2), pp. 138–147, DOI:
462 10.1016/j.cryobiol.2007.06.005.
- 463 [31] Xu F., Moon S., Zhang X., Shao L., Song Y.S., Demirci U., Multi-scale heat and mass
464 transfer modelling of cell and tissue cryopreservation, *Philosophical Transactions of the*
465 *Royal Society A: Mathematical, Physical and Engineering Sciences*, 2010, 368(1912),
466 pp. 561–583, DOI: 10.1098/rsta.2009.0248.
- 467 [32] Youn J.-I. *et al.*, Optical and thermal properties of nasal septal cartilage, *Lasers in*
468 *Surgery and Medicine*, 2000, 27(2), pp. 119–128, DOI: 10.1002/1096-
469 9101(2000)27:2<119::AID-LSM3>3.0.CO;2-V.
- 470 [33] Yu X., Zhang S., Chen G., Modeling the addition/removal of dimethyl sulfoxide
471 into/from articular cartilage treated with the liquidus-tracking method, *International*
472 *Journal of Heat and Mass Transfer*, 2019, 141, pp. 719–730, DOI:
473 10.1016/j.ijheatmasstransfer.2019.07.032.
- 474 [34] Zadeh L.A., Fuzzy sets, *Information and Control*, 1965, 8(3), pp. 338–353.
- 475 [35] Zhao G., Fu J., Microfluidics for cryopreservation, *Biotechnology Advances*, 2017,
476 35(2), pp. 323–336, DOI: 10.1016/j.biotechadv.2017.01.006.
- 477